Fragmentation Behavior of Silica-Supported Metallocene/MAO Catalyst in the Early Stages of Olefin Polymerization

Xuejing Zheng, Madri Smit, John C. Chadwick, and Joachim Loos*

Department of Chemical Engineering and Chemistry, and Dutch Polymer Institute, Eindhoven University of Technology, P.O. Box 513, 5600MB, Eindhoven, The Netherlands

Received February 9, 2005; Revised Manuscript Received April 4, 2005

ABSTRACT: Polymer particle growth in the early stages of olefin polymerization has been investigated using metallocene/methylaluminoxane (MAO)/silica catalyst systems. Scanning electron microscopy (SEM) has been used to characterize the surface and cross-sectional morphology of polymer particles at different stages of particle growth. The aluminum distribution in various MAO-impregnated supports has been determined by energy-dispersive X-ray (EDX) analysis, revealing that the homogeneity of the distribution is dependent on both the silica calcination temperature and the impregnation conditions used. Depending on the impregnation routes and polymerization conditions applied, two fragmentation behaviors have been observed: main polymerization at the surface with coarse fragmentation at the core of the support particles in the case of propylene polymerization and a heterogeneous (co)catalyst distribution, and a layer-by-layer fragmentation of the support in ethylene polymerization using a homogeneously immobilized catalyst.

Introduction

The discovery of metallocene/organoalumoxane (especially methylaluminoxane, MAO) catalysts for olefin polymerization has opened up new frontiers in the area of organometallic chemistry and polymer synthesis.[1] High catalyst activity and the synthetic accessibility of tailor-made polymers having well-defined microstructures and narrow molar mass distributions represent the main advantages of metallocene catalysts in comparison to classical Ziegler−Natta or Phillips catalysts. However, being homogeneous catalysts, those systems present disadvantages in regard to their industrial application in polyolefin slurry or gas-phase processes. One approach to overcome this problem is the immobilization of such catalyst systems (metallocene/MAO) by physically or chemically supporting them on the surface of a solid carrier.[2−5]

The major objective of catalyst immobilization is to preserve the advantages of a homogeneous catalyst in terms of the high activity and the control over polymer microstructure and at the same time to provide acceptable polymer particle morphology to prevent reactor fouling and give high bulk density. Controlled fragmentation of the initial support particles is an important factor here.[2−5] Immobilization has increased the complexity of metallocene-catalyzed systems, as it has added the influence of the support and the supporting method. Supports with high specific surface area are commonly used since they maximize the number of accessible active sites per unit volume. The catalyst carrier has to be relatively stable to avoid disintegration and polymer fines formation, but on the other hand, it has to be able to fragment, under the hydraulic forces of the growing polymer, into submicron primary particles which become dispersed throughout the polymer granule. These small particulate residues from the support should not disturb the processing of the polymer.

Amorphous SiO_2 has generally been the preferred support for metallocene immobilization. In addition to controlling polymer morphology, silica's unique surface chemistry, namely, the concentration and strength of hydroxyl groups and siloxane bridges, can be used to immobilize reagents. The amount and type of surface functional groups of silica promotes further control in these heterogeneous systems. The unique characteristics of metallocene systems, combined with those of silica, facilitate the formation of uniform polymer particles with narrow particle size distributions and high bulk densities.[5,6]

Examination of the literature suggests that there are three basic methods of immobilization: (1) tethering of the metallocene to the silica surface and then reacting with MAO solution; (2) the reaction of the cocatalyst MAO with the hydroxyl surface of the silica gel, followed by impregnation with the metallocene; (3) a one-step impregnation of a preactivated MAO/metallocene complex.[2,5−8] MAO is expected to chemically link to the silica support, and the activated metallocene cation will in turn be bound to the supported MAO by means of electrostatic interactions. The interaction of an immobilized catalyst system with the support material is of great importance since this will strongly determine the possibility of leaching.[5,9,10]

Next to the immobilization strategy, the polymerization conditions chosen determine the extent of the fragmentation behavior and the replication of the polymer particle. Slurry polymerization in an organic diluent gives important insights into polymerization kinetics even at low conversion.[11] This arises from mild reaction conditions, making use of low temperature, pressure, catalyst concentration, and/or monomer concentration. Lowering the polymerization temperature facilitates an investigation of the polymer growth in the early stages of polymerization and the development of particle growth models for heterogeneous metallocene/MAO catalyst systems based on silica. The low reaction rates allow full activation of the catalyst and lead to a controlled fragmentation of the catalyst.[12,13] The morphology of the polymer particles may be very complex, and understanding the fragmentation behavior repre-

* Corresponding author. E-mail: j.loos@tue.nl.

10.1021/ma0502912 CCC: $30.25
Published on Web 04/30/2005

sents an important research task. Good spherical morphology, controlled porosity, and narrow particle size distribution are essential features of any catalyst used in a polyolefin slurry or gas-phase process.

It is generally agreed that the final particle morphology is strongly dependent on the initial fragmentation stage.[3,13−16] However, limited data appear to be available concerning the distribution of the active sites in the supported catalyst, the mechanism and rate by which the catalyst fragmentation proceeds, and the distribution of the fragments throughout the polymer particle. In particular, there is a need for further knowledge about the phenomena occurring in the early stages of the polymerization.

In the present work, different approaches have been used for immobilization of the cocatalyst (MAO) and catalyst on a silica support. Olefin polymerization was carried out in heptane slurry under very mild conditions and stopped at low yield, expressed as grams of polymer per gram catalyst (support included). The surface and cross-sectional morphologies of the polymer particles were characterized by scanning electron microscopy, enabling us to monitor the support fragmentation behavior and polymer particle growth in the very early stage of the polymerization. The distribution of immobilized MAO in the support was characterized by energy-dispersive X-ray analysis.

Experimental Section

Materials. Silica support materials, Sylopol 948 (Grace AG) and MS-3040 (PQ Corp.), were kindly donated by their respective suppliers. Characteristics of the supports such as particle size and porosity can be found in ref 17. A 10 wt % solution of the cocatalyst methylaluminoxane (MAO) in toluene was obtained from Witco, while *racemic* ethylene-bridged bis(indenyl)zirconium dichloride (*rac*-Et(Ind)$_2$ZrCl$_2$) was purchased from STREM chemicals. Triisobutylaluminum (TIBA) was obtained from Akzo Nobel as a 25 wt % solution in toluene. Ethylene (Air Liquide) and propylene (Hoekloos) were dried over columns containing activated copper catalyst (BTS) and alumina before introduction into the polymerization reactor.

MAO Immobilization. Before immobilizing MAO on the support, the silica materials were calcined in a calibrated oven at 250 or 600 °C, under a N_2/O_2 (3:1) flow. The silica was heated at 15 °C/min until the desired temperature was reached and then held isothermally at that temperature for 3 h, after which the sample was allowed to cool to ambient temperature.

Three different immobilization procedures (denoted as methods I, II, and III) were used:

Method I: In this first approach, 1 g of calcined silica was slurried in 5 mL of toluene and contacted with 3.12 mmol of MAO (10 wt % in toluene, diluted with a further 5 mL of toluene) at room temperature over a period of 5 min. The slurry was left for 2 h, after which it was washed with 10 mL of *n*-heptane and dried under vacuum to obtain a free-flowing powder.

Method II: In this more rigorous impregnation method, the silica/MAO slurry in toluene was heated to 110 °C and kept at this temperature for 4 h. After allowing to cool to ambient temperature, the solid was separated from the solvent by decantation and was contacted with 5 mL of fresh toluene at 90 °C for 45 min. This procedure was repeated, after which the solvent was again decanted, and the solid support was dried at 120 °C and 22 mbar for 1 h to give a free-flowing powder.

Method III: In this approach, using Sylopol 948 calcined at 600 °C, the zirconocene (2.39 μmol) and MAO (3.12 mmol; 10 wt % solution in toluene) were mixed for 10 min and added over 10 min to silica (1 g) in toluene (1.5 mL) at 0 °C. After a further 10 min, the temperature was gradually increased under reduced pressure (22 mbar) to 63 °C, over a period of 5 h, to give a free-flowing powder.

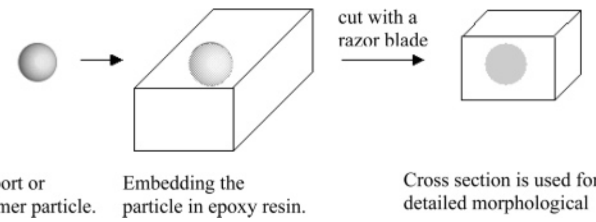

Figure 1. Scheme of particle cross-section preparation.

Polymerization Procedure. Polymerizations were carried out at 50 °C in a 200 mL Büchi glass reactor or a 1 L Premex stainless steel reactor. Both reactors were fitted with a hollow-shaft turbine stirrer. TIBA was used as scavenger, while *n*-heptane was used as polymerization medium. MAO-impregnated supports prepared by methods I and II were used in 100 mg quantities and first contacted for 1 h with a solution of the activated catalyst prepared by dissolving the zirconocene (2.39 μmol) in 1 mL of toluene and 1.8 mmol of TIBA (25 wt % solution in toluene) and standing for 1 h. Ethylene and propylene were used for polymerizations at the monomer pressure of 2.5 and 4 bar, respectively. The polymerization was terminated by monomer degassing, followed by quenching with acidic methanol.

More detailed information on immobilization and polymerization procedures used can be found in refs 17 and 18.

Characterization of Particle Morphology. The surface and cross-sectional morphologies of the samples were investigated using a Philips environmental scanning electron microscope XL-30 ESEM FEG (Philips, The Netherlands, now Fei Co.) equipped with an energy-dispersive X-ray spectrometer (EDX) for local and area distribution analyses of elements. Imaging of the samples surfaces and cross sections was performed in high-vacuum mode using acceleration voltages of 1 kV (low-voltage SEM, LVSEM) and a secondary electron (SE) detector. Qualitative EDX analysis was carried out under controlled N_2 atmosphere at an accelerating voltage of 20 kV. Some samples were imaged at this condition using the gaseous secondary electron detector (GSED). No additional coating of the sample surface was done because charging is not an issue for the chosen imaging conditions. For the investigation of cross sections, the catalyst and polymer particles were embedded in SPURR low-viscosity epoxy resin (SPI Supplies) and cut with a razor blade after cooling the sample in liquid nitrogen. The cross-section procedure is illustrated in Figure 1.

Results and Discussion

Catalyst Distribution on Silica Supports. Energy-dispersive X-ray analysis is a powerful and convenient method to study catalyst immobilization.[2,19] The homogeneity of the distribution of catalytic components on the support can be determined by EDX element analysis of bulk cross sections. We found that the weight percentage of Al in our MAO-impregnated support is typically around 7−11% and, therefore, is easily detectable with EDX analysis. With a weight percentage of about 0.1−0.3%, the Zr concentration, however, is distinctly lower than the detection limit and cannot be directly determined.

Figure 2 shows the EDX analysis of a cross section of MAO-impregnated support particles prepared using silica (Sylopol 948) calcined at two different temperatures. Impregnation was carried out by simple treatment of the calcined silica with a solution of MAO in toluene at ambient temperature, as described in the Experimental Section (method I). The EDX mappings reveal that the silica calcined at 250 °C gave a core−shell Al distribution, indicating a relatively high con-

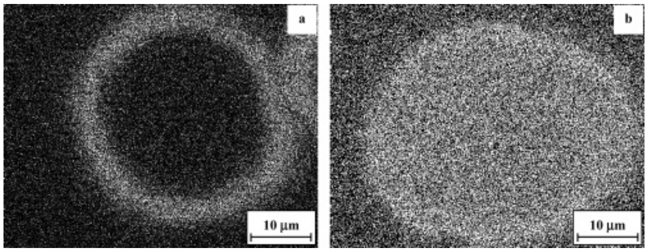

Figure 2. Al mappings of silica/MAO particle cross-section (MAO immobilization method I) calcined at (a) 250 and (b) 600 °C. High brightness reflects high Al concentration.

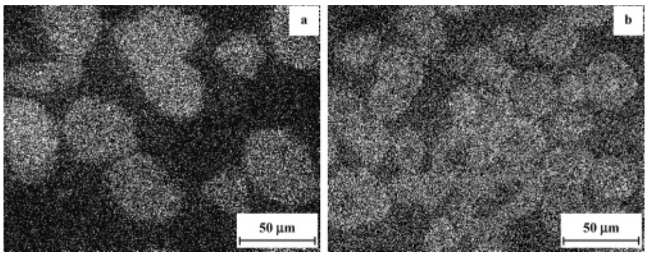

Figure 3. Al mappings of silica/MAO particle cross-section (MAO immobilization method II) calcined at (a) 250 and (b) 600 °C. High brightness reflects high Al concentration.

centration of MAO at and near the particle surface, but very little in the particle interior (Figure 2a). However, a much more homogeneous MAO distribution is evident (Figure 2b) in the support prepared after calcination of the silica at 600 °C. The effect of calcination temperature in this simple impregnation of silica with MAO may reflect the effect of the different silanol contents, 3.2 and 1.4 mmol/g, after calcination at 250 and 600 °C, respectively.[17] The higher residual silanol content in the silica calcined at 250 °C would be expected to aid the chemical fixation of MAO and slow diffusion of MAO into the particle would therefore lead to its immobilization predominantly on or near the particle surface.

Figure 3 shows the EDX Al mappings of cross sections of support/MAO particles made by the more rigorous impregnation of silica with MAO at elevated temperatures (method II). It is seen that MAO is homogeneously distributed on the support as a result of improved penetration. Even after calcination at 250 °C, it is apparent that, despite the higher concentration of OH groups on the silica surface, the MAO has completely penetrated into the mesopores of the silica, without formation of a concentration gradient.

Support Fragmentation Behavior and Polymer Particle Growth. Ferrero, Chiovetta, Fink, and others have contributed to a great extent to the understanding of polyolefin particle growth using supported catalysts.[2,19−25] Fink and co-workers focused on SiO_2-supported metallocene catalyst systems. In slurry polymerization experiments carried out under mild conditions, they observed an induction period during which a continuous filling of the catalyst pores with polymer from the outside to the interior areas takes place. In this initial phase, no polymer is formed at the center of the particle, support fragmentation induced by the hydraulic force of the growing polymer being incomplete. The induction period is followed by continuous fragmentation to release new active centers, resulting in an increase in activity and leading to the main polymerization phase. The fragmentation of catalyst can be described as “layer-by-layer”, from the external surface to the center of the macroparticle, until all the catalyst is fragmented. However, a different particle growth mechanism has been observed using $MgCl_2$-supported catalysts. In propylene polymerizations using Ziegler−Natta catalysts, Noristi et al.[16] and Pater et al.[12] have observed rapid fragmentation of the catalyst into a great number of small subparticles, which are kept together by the growing polymer. Each fragment acts as a nucleus around which further polymer growth occurs. The fragments remain entrapped and dispersed in the growing polymer mass and move outward in proportion to the local volumetric expansion due to polymerization. Cecchin et al.[15] have described a particle growth model

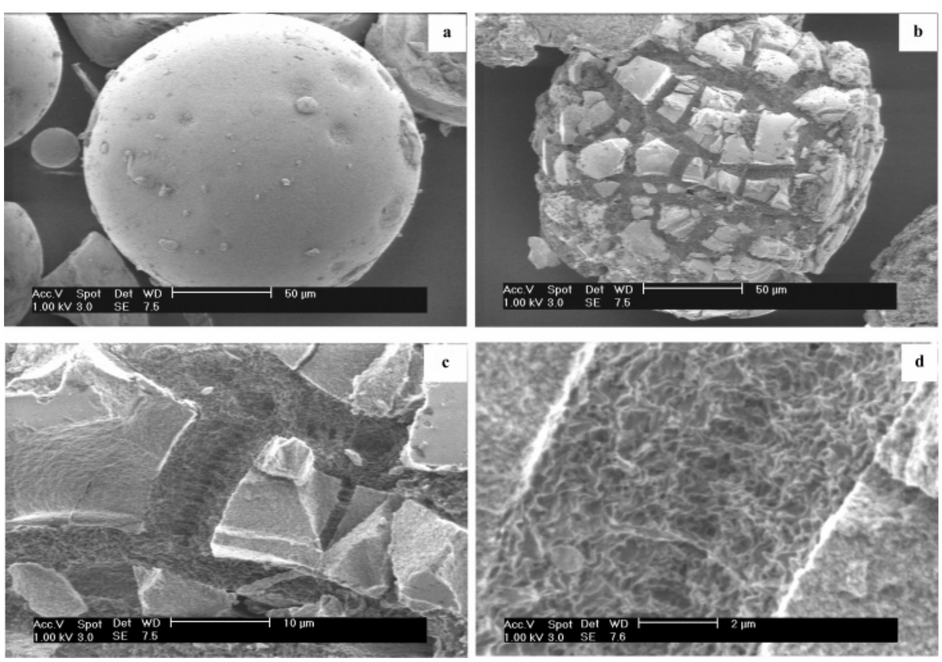

Figure 4. LVSEM images of (a) a typical silica/MAO particle and a polypropylene particle at the yield of 1.8 g of polymer per gram of catalyst (MAO immobilization method II), (b) overview, same magnification as (a), (c) details of fragmentation, and (d) details of polymer growing between fragments.

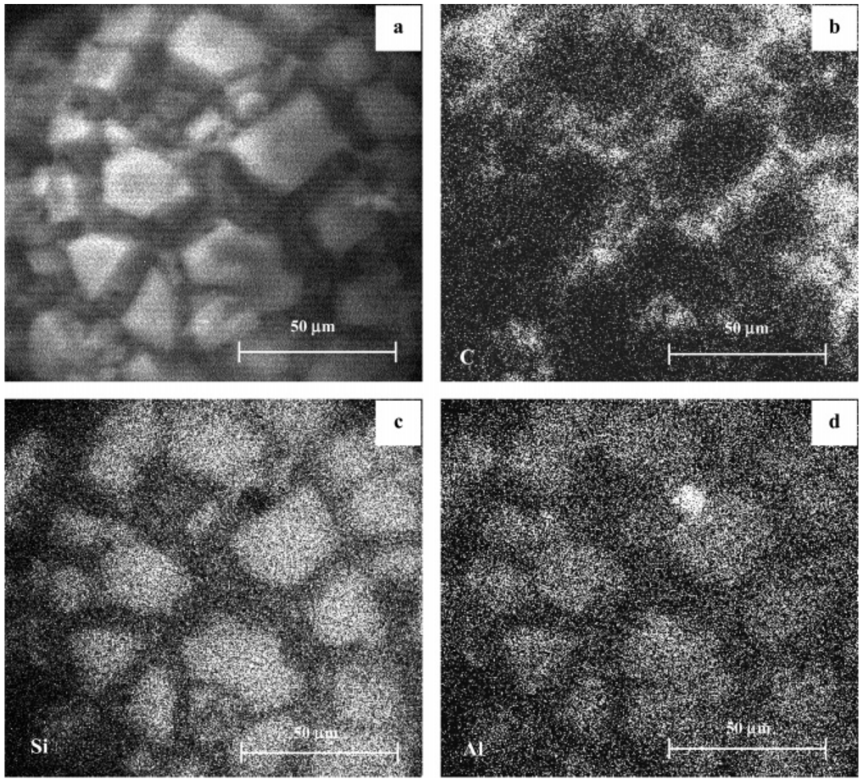

Figure 5. Element distribution mappings of surface image of a polypropylene particle at the early stage of polymerization: (a) GSED image of the particle, (b) carbon mapping, (c) silica mapping, and (d) aluminum mapping.

in which agglomerates of primary catalyst crystallites give rise to the formation of subglobules of polymer within the growing particle.

In the present work, particle fragmentation and replication behavior were first studied after a simple impregnation of silica with MAO and contact of the resulting support with the metallocene prior to polymerization (method I). Propylene polymerization was carried out using a catalyst with very low activity in heptane slurry for 1 h at the temperature of 50 °C and the monomer pressure of 4 bar.[17] The polymer with very low yield (1.8 g of polymer per gram of catalyst) was obtained. The surface images of a polymer particle are shown in Figure 4. It is seen from Figure 4b that the outer surface of the polymer particle is composed of fragmented silica support (brighter phase) and freshly formed polymer (dark phase). At higher magnification, silica is seen to be broken into irregular subparticles with a diameter of 5−20 μm (Figure 4c). The catalyst particle does not lose its overall integrity because the individual fragments are held together by the polymer formed (Figure 4d). The EDX analysis of the polymer particle is shown in Figure 5. One can assign the individual phases in the SEM micrograph by means of elemental mappings. The bright parts in Figure 5b represent carbon-rich areas, which consist mainly of polymer. The bright parts in Figure 5c and d represent Si and Al, respectively, which are from silica support and immobilized cocatalyst MAO. It can be seen that the driving force of the support fragmentation is the polymer growth. The initial fragmentation of the catalyst at the early stage of polymerization can be interpreted as seen in the scheme of Figure 6. It shows that the catalyst fragmentation starts at the very beginning of the polymerization. In other words, a very small amount of polymer is sufficient to break the catalyst into subgrains, illustrating how the hydraulic force of the polymer formed in the pores of the silica can fragment the support.

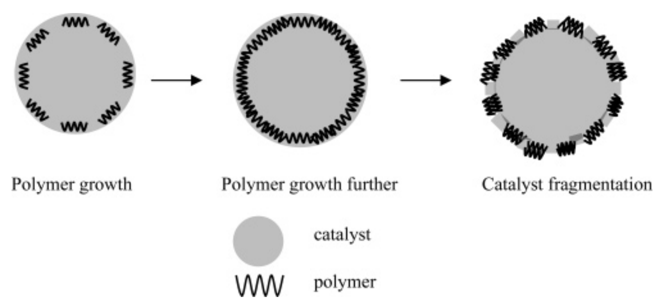

Figure 6. Scheme of catalyst fragmentation at the very early stages of polymerization.

In Figure 7 a series of images are presented that show polyethylene particle growth and replication behavior with increasing polymerization time. Here, catalyst and MAO impregnation on the support was carried out by contacting silica (Sylopol 948, calcined at 600 °C) with a precontacted mixture of *rac*-Et(Ind)$_2$ZrCl$_2$ and MAO in a small volume of toluene so as to facilitate pore filling, aiming at homogeneous impregnation of both MAO and zirconocene on the support. At low yield (2.7 g/g), the polymer particle surface reveals a cauliflower morphology (Figure 7d,e). The surface of the particle becomes rough, comprising subgrains with diameter of 2−20 μm. The cross section (Figure 7f) indicates that the polymerization first takes place on the outer part of the particle, while the center of the support remains unfragmented. At higher yield (10.7 g/g), it is shown in Figure 7g,h that the size of the polymer particle increases further. The surface of the polymer particle is composed of many small subgrains, while unfragmented silica is still visible at the particle center. After further polymerization, leading to a yield of 33.2 g/g, the surface image of a polymer particle at high magni-

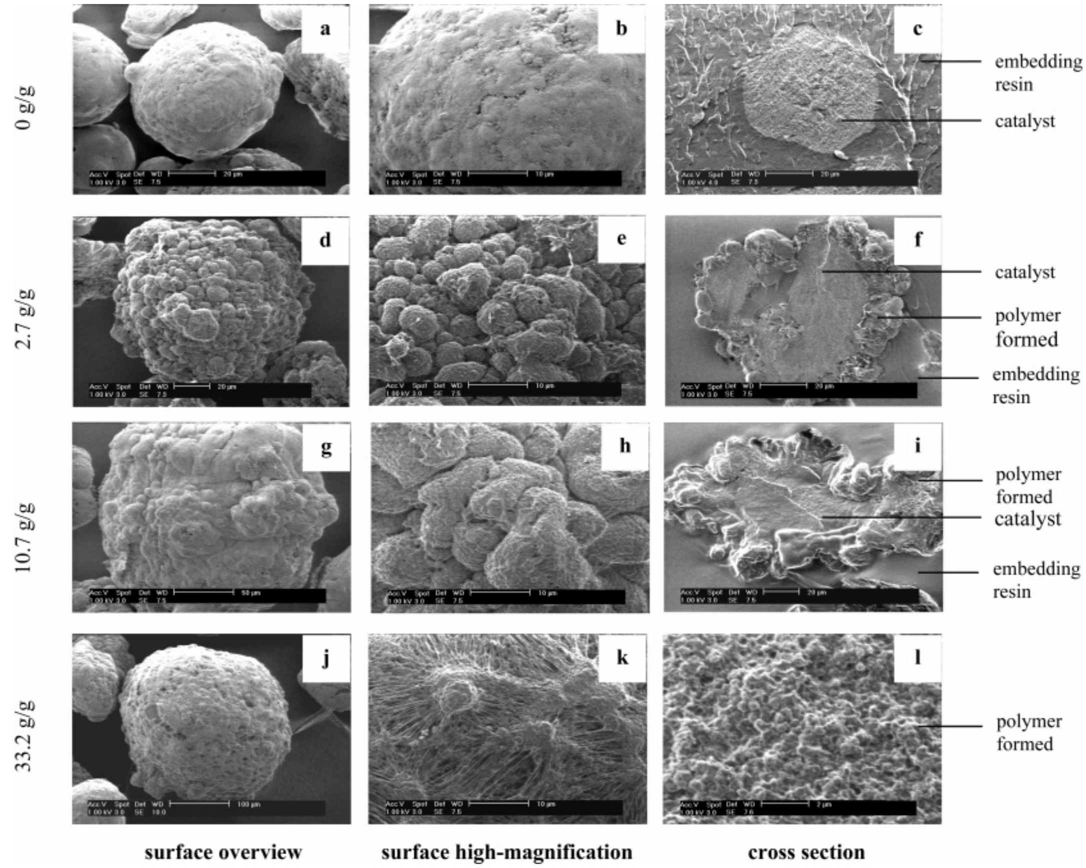

Figure 7. LVSEM surface and cross-section images of polyethylene particles at different yield, expressed in grams of polymer per gram of catalyst (MAO immobilization method III).

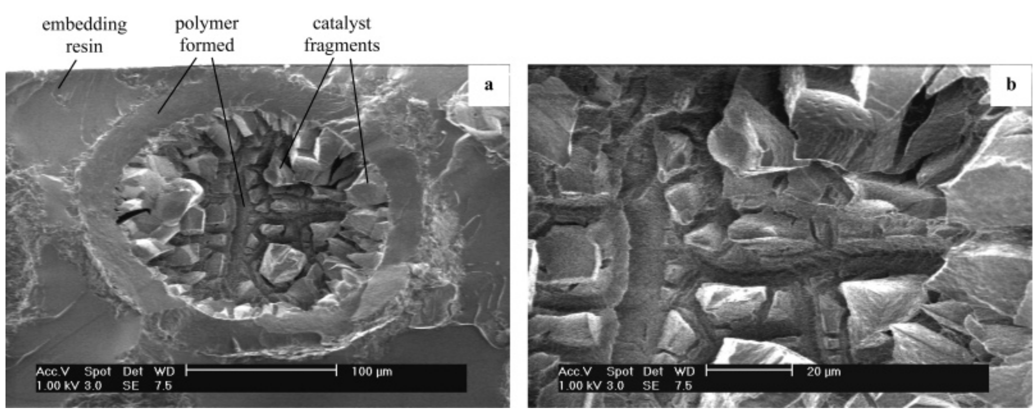

Figure 8. LVSEM images of the cross-section morphology of a PP polymer particle at yield of 8.5 g of polymer per gram of catalyst (MAO immobilization method I): (a) overview and (b) high magnification.

fication (Figure 7k) shows that the polymer particle is composed of subgrains with diameter of about 5−10 μm, while the smaller domains from which the subgrains are made up can clearly be recognized. The polymer subgrains are linked by fibrils, formed by particle growth. The cross-section image in Figure 7l shows that the polymer particle is composed of microparticles with diameter less than 500 nm. It seems that the density of the microparticles is higher in the core than at the surface, and no fibrils are found. This is a clear indication that the fibrils are formed by expansion during the growth of the polymer particle. The original silica support is so finely divided that it is almost impossible to find residues within the polymer particle by SEM. The observed catalyst fragmentation behavior can be described as layer-by-layer. The polymerization starts at the active sites on the surface of the support. On the outer surface of the silica, and to some degree below the surface, a thin polymer boundary layer is formed during the initial stage. When sufficient monomer has diffused through the outer polymer layer to reach the active centers inside the particle, further polymer growth starts, and the evolved hydraulic pressure exerted by the polymer being formed causes further fragmentation and the formation of polymer subgrains.

A very different type of fragmentation behavior was observed in propylene polymerization after catalyst immobilization carried out according to method 1, as described in the Experimental Section. In this case, a MAO-impregnated silica was used in which most of the MAO present was concentrated at or near the particle surface. The cross-sectional images of the resulting polymer (Figure 8) reveal a dense polymer skin with a thickness of about 20 μm, while many support fragments are visible within the otherwise hollow particle interior. In this case, it appears that the support immediately breaks up into a great number of subparticles, which are kept together by the growing polymer. Instantaneous catalyst fragmentation behavior is well reported in work based on $MgCl_2$-supported Ziegler–Natta catalyst systems[12,16] but is less well-known in silica-supported metallocene/MAO catalyst systems. Evidently, the dense polymer growth at the particle surface is sufficient to cause a coarse fragmentation of the support at the center of the particle, despite negligible polymer formation in the particle interior.

Conclusions

Energy-dispersive X-ray analysis is demonstrated to be a very useful method to characterize the catalyst distribution on a support material. A core–shell or homogeneous distribution of MAO on silica support can be obtained, dependent on the supporting method used. Uniform impregnation of a silica support with MAO is difficult to achieve simply by contacting the support with MAO in toluene at ambient temperature. Homogeneous impregnation of MAO on a silica support was achieved by a more rigorous impregnation of silica with MAO at elevated temperatures. Scanning electron microscopic studies of the polymer morphology and the fragmentation of the support reveal two kinds of fragmentation behaviors: a layer-by-layer fragmentation and an instantaneous breakup of the support, dependent on (co)catalyst distribution on the support, the monomer (ethylene or propylene) used, and the polymerization conditions applied. Further work on the influence of catalyst preparation and polymerization conditions on the fragmentation behavior is currently in progress.

Acknowledgment. The authors gratefully acknowledge support from Dutch Polymer Institute for Projects #331 and #111.

References and Notes

(1) Kaminsky, W. *J. Polym. Sci., Part A: Polym. Chem.* **2004**, *42*, 3911.

(2) Fink, G.; Steinmetz, B.; Zechlin, J.; Przybyla, C.; Tesche, B. *Chem. Rev.* **2000**, *100*, 1377.

(3) McKenna, T. E.; Soares, J. B. P. *Chem. Eng. Sci.* **2001**, *56*, 3931.

(4) Hlatky, G. G. *Chem. Rev.* **2000**, *100*, 1347.

(5) Duchateau, R. *Chem. Rev.* **2002**, *102*, 3525.

(6) Galland, G. B.; Seferin, M.; Guimaraes, R.; Rohrmann, J. A.; Stedile, F. C.; dos Santos, J. H. Z. *J. Mol. Catal. A: Chem.* **2002**, *189*, 233.

(7) Estenoz, D. A.; Chiovetta, M. G. *J. Appl. Polym. Sci.* **2001**, *81*, 285.

(8) Alt, H. G. *J. Chem. Soc., Dalton Trans.* **1999**, 1703.

(9) Chang, M. US Patent 5,008,228, 1991.

(10) Kutschera, D.; Rieger, R. US Patent 5,789,332, 1998.

(11) Steinmetz, B.; Tesche, B.; Przybyla, C.; Zechlin, J.; Fink, G. *Acta Polym.* **1997**, *48*, 392.

(12) Pater, J. T. M.; Weickert, G.; Loos, J.; van Swaaij, W. P. M. *Chem. Eng. Sci.* **2001**, *56*, 4107.

(13) Weickert, G.; Meier, G. B.; Pater, J. T. M.; Westerterp, K. P. *Chem. Eng. Sci.* **1999**, *54*, 3291.

(14) Weist, E. L.; Ali, A. H.; Naik, B. G.; Curtis Conner, Wm. *Macromolecules* **1989**, *22*, 3244.

(15) Cecchin, G.; Marchetti, E.; Baruzzi, G. Maromol. *Chem. Phys.* **2001**, *202*, 1987.

(16) Noristi, L.; Marchetti, E.; Baruzzi, G.; Sgarzi, P. *J. Polym. Sci., Part A: Polym. Chem.* **1994**, *32*, 3047.

(17) Smit, M.; Zheng, X.; Loos, J.; Chadwick, J. C. *J. Polym. Sci., Part A: Polym. Chem.,* in press.

(18) Smit, M.; Zheng, X.; Loos, J.; Chadwick, J. C. Manuscript in preparation.

(19) Zechlin, J.; Steinmetz, B.; Tesche, B.; Fink, G. *Macromol. Chem. Phys.* **2000**, *201*, 515.

(20) Ferrero, M. A.; Chiovetta, M. G. *Polym. Eng. Sci.* **1987**, *27,* 1448.

(21) Ferrero, M. A.; Chiovetta, M. G. *Polym. Eng. Sci.* **1991**, *31*, 886.

(22) Ferrero, M. A.; Chiovetta, M. G. *Polym. Eng. Sci.* **1987**, *27,* 1436.

(23) Ferrero, M. A.; Chiovetta, M. G. *Polym. Eng. Sci.* **1991**, *31*, 904.

(24) Bonini, F.; Fraaije, V.; Fink, G. *J. Polym. Sci., Part A: Polym. Chem.* **1995**, *33*, 2393.

(25) Knoke, S.; Korber, F.; Fink, G.; Tesche, B. *Macromol. Chem. Phys.* **2003**, *204*, 607.

MA0502912